

ESI for: 2-Bromo perylene diimide: synthesis using C–H activation and use in the synthesis of bis(peryene diimide)-donor electron-transport materials

Junxiang Zhang,^a Sanjeev Singh,^b Do Kyung Hwang,^b Stephen Barlow,^a Bernard Kippelen,^b and Seth R. Marder^a

^aSchool of Chemistry and Biochemistry, ^bSchool of Electrical and Computer Engineering, and Center for Organic Photonics and Electronics, Georgia Institute of Technology, Atlanta, GA 30332, United States.

Supporting Information

Contents

1. Materials and General Methods
2. DFT molecular geometry optimisation
3. Electrochemical Properties
4. Thermal characterisation
5. OFETs fabrication and device properties
6. X-ray characterisation of films
7. NMR Spectra of New Compounds

1. Materials and General Methods

^1H and $^{13}\text{C}\{^1\text{H}\}$ NMR spectra were acquired using a Bruker AMX-400 spectrometer or Varian Mercury Vx 300, and the signals were referenced to residual solvent peak (7.27 ppm for ^1H NMR and 77.0 ppm for ^{13}C NMR) or internal standard TMS (0.0 ppm).

Chromatographic separations were performed using standard flash column chromatography methods using silica gel purchased from Sorbent Technologies (60 Å, 32-63 µm). Electrochemical measurements were carried out under nitrogen in dry deoxygenated 0.1 M tetra-*n*-butylammonium hexafluorophosphate in dichloromethane (ca. 10^{-4} M of analyte) using a conventional three-electrode cell with a glassy carbon working electrode, platinum wire counter electrode, and a Ag wire coated with AgCl as pseudo-reference electrode. Potentials were referenced to ferrocenium/ferrocene. Cyclic voltammograms were recorded at a scan rate of 50 mV.s $^{-1}$. UV-vis-NIR spectra were recorded in 1 cm cells using a Varian Cary 5E spectrometer. Mass spectra were recorded on an Applied Biosystems 4700 Proteomics Analyzer by the Georgia Tech Mass Spectrometry Facility. Elemental analyses were performed by Atlantic Microlabs. Differential scanning calorimetry measurements were taken on a Q200 Differential Scanning Calorimeter (TA Instruments, New Castle, DE), at 10 °C min $^{-1}$, with 50 mL min $^{-1}$ N $_2$ flow, with total organic solids weight of ca. 5 mg.

Table 1. Conditions tried for the Ir- or Ru-catalysed direct monoborylation of **PDI**

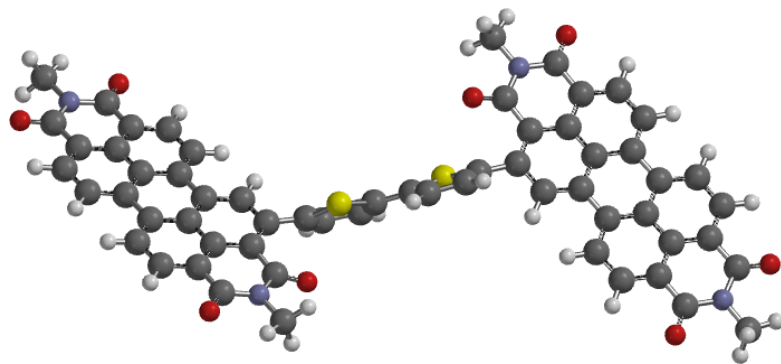
Entry	TM Catalyst	B $_2$ Pin $_2$	Solvent	Temperature (°C)	Yield of PDI-Bpin (isolated)
1	[Ir(OMe)cod] $_2$ ^a (3 mol%) P(C $_6$ F $_5$) $_3$ (12 mol%)	1.5 eq	dioxane	120	35%
2	[Ir(OMe)cod] $_2$ (3 mol%) P(C $_6$ F $_5$) $_3$ (12 mol%)	1.0 eq	dioxane	110	~11%
3	[Ir(OMe)cod] $_2$ (3 mol%) P(C $_6$ F $_5$) $_3$ (12 mol%)	2.0 eq	dioxane	110	~12%
4	Ru(H) $_2$ (CO)(PPh $_3$) $_3$ (50 mol%)	8.0 eq	mesitylene/pinacolone	140	44%
5	RuH $_2$ (CO)(PPh $_3$) $_3$ (10 mol%)	1.2 eq	mesitylene/pinacolone	140	38%

^a cod = 1,5- cyclooctadiene

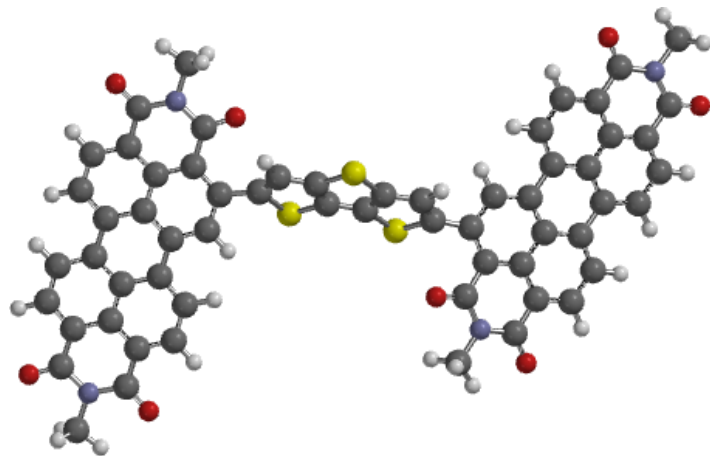
2. DFT molecular geometry optimisation

The neutral ground-state structures were obtained at the DFT (B3LYP/6-31G**) level for **7-9** and **PDI2-DTP-bay** with all *N,N'*-alkyl groups replaced by methyl groups to reduce computational cost.

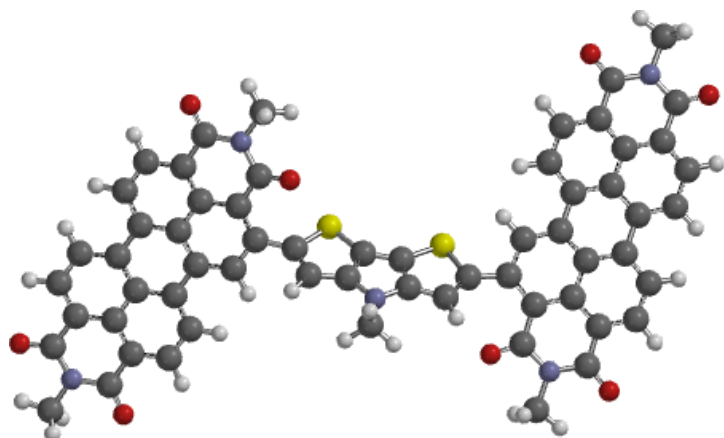
7



8



9



10

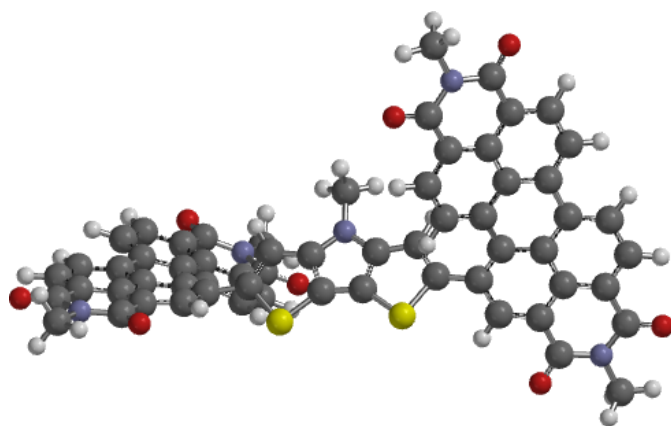


Figure S1. DFT-predicted (B3LYP/6-31G* level) conformations (side view) of **7-10**.

3. Electrochemical Properties

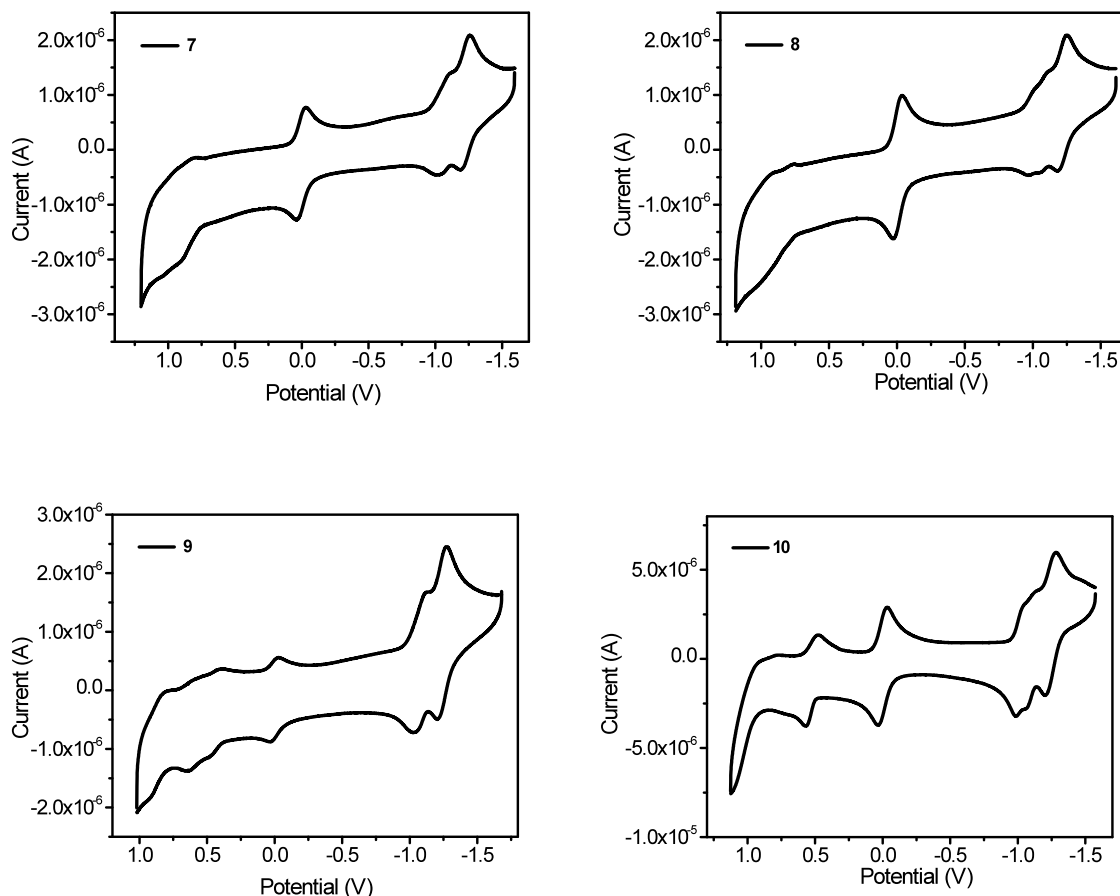


Figure S2. Cyclic voltammograms of **7-10** conducted in 0.1 M $n\text{Bu}_4\text{NPF}_6$ in CH_2Cl_2 with $\text{Cp}_2\text{Fe}^{+/0}$ as internal reference at a scan rate of 50 mV s^{-1} .

4. Thermal Characterisation

Differential scanning calorimetry (DSC, Figure S3) indicating melting points of ca. 248.5°C and 260.3°C for **7** and **8**, respectively; this indicates that the materials possess enough thermal stability for applications in thin film devices. Upon cooling, two corresponding exothermic transitions are observed at 243.5°C and 219.2°C , respectively. **9** solid shows no visible thermal transitions up to 350°C .

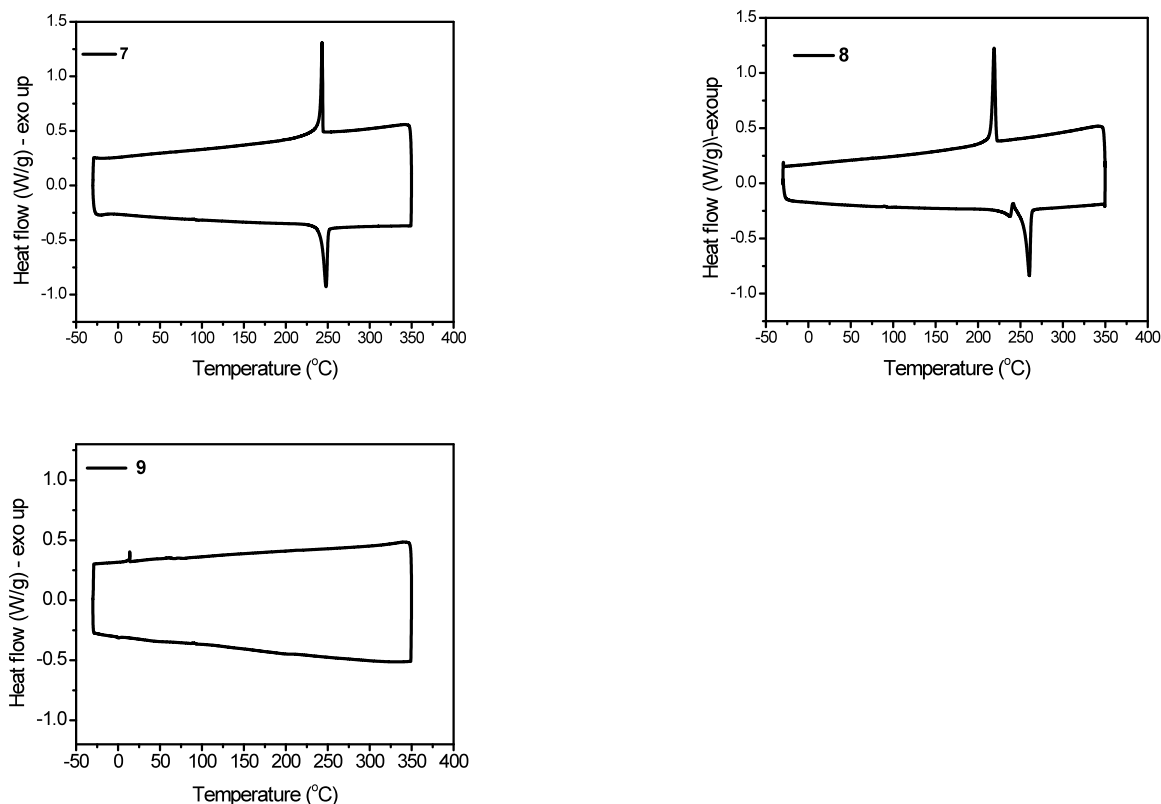


Figure S3. Second scanning differential scanning calorimetry plots of compounds **7**, **8**, and **9**.

5. OFET Fabrication and Properties

OFETs with bottom contact and top gate structure were fabricated on glass substrates (Eagle 2000 Corning). Au (50 nm) bottom contact source/drain electrodes were deposited by thermal evaporation through a shadow mask. Organic semiconductor layers were formed on the substrates by spin coating solution of **7-9** ($10\text{--}15\text{ mg mL}^{-1}$) at 500 rpm for 10 s and at 2000 rpm for 20 s. These organic layers were annealed at 100 °C for 15 min on the hot plate inside a nitrogen glove box. CYTOP (45 nm)/Al₂O₃ (50 nm) bilayers was used as top gate dielectrics. CYTOP solution (CTL-809M) was purchased from Asahi Glass with a concentration of 9 wt. %. To deposit the 45-nm-thick fluoropolymer layers, the original solution was diluted (CT-solv.180, Asahi glass) to give solution:solvent ratios of 1:3.5. CYTOP layers were deposited by spin coating at 3000 rpm for 60 s. Al₂O₃ (50 nm) films were deposited on fluoropolymer layers by atomic layer deposition at 110 °C using alternating exposures of AlMe₃ and H₂O vapor at a deposition rate of approximately 0.1 nm per cycle. All spin coating and annealing processes were carried out in a N₂-filled dry box. Finally, Al (150 nm) gate electrodes were deposited by thermal evaporation through a shadow mask.

Bottom gate and top contact OFETs were fabricated on heavily doped n-type silicon substrates (resistivity $< 0.005 \Omega\text{cm}$, also serve as gate electrodes) with 200 nm thick thermally grown SiO_2 as the gate dielectric. Firstly, the substrates were cleaned by O_2 plasma for two minutes. The SiO_2 dielectric surface was then passivated with a thin buffer layer of BCB (CycloteneTM, Dow Chemicals), to provide a high-quality hydroxyl-free interface. The BCB was in diluted in trimethylbenzene with the ratio 1:20, and spincoated at 3000 rpm for 60 s to provide a very thin uniform layer (thickness was not measured, final capacitance density was measured). The samples were annealed at 250 °C for 1 h inside a N_2 glove box for crosslinking. The total capacitance density (C_{OX}) was measured from parallel-plate capacitors; it was found to be ca. 14.5 nF/cm^2 . An organic layer was spin coated (500 rpm for 10 s and 2000 rpm for 20 s) from solutions of **7-9** ($10 - 17 \text{ mg mL}^{-1}$) in designated solvents. Finally, Al (150 nm) was deposited through a shadow mask to act as source/drain electrodes.

All current-voltage (I-V) characteristics of OFETs were measured with an Agilent E5272A source/monitor unit in a N_2 -filled glove box (O_2 , $\text{H}_2\text{O} < 0.1 \text{ ppm}$).

Table S2. Summary of top-gate bottom-contact OFETs and bottom-gate top-contact OFETs

<i>Compound</i>	C_{in} (nF cm^{-2})	Solvent	S/D electrode	μ ($\text{cm}^2 \text{V}^{-1} \text{s}^{-1}$)	V_{TH} (V)	$I_{\text{on/off}}$
8^a	35.2	DCB	Au	$1.27(\pm 0.04) \times 10^{-2}$	4.2 ± 0.5	5×10^3
7^a	35.2	CHCl_3	Au	$2.9(\pm 0.7) \times 10^{-3}$	$4.9(\pm 0.6)$	1×10^3
7/PS^a (1:1)	35.2	DCB	Au/Ti	$2.4(\pm 1.7) \times 10^{-2}$	$5(\pm 1)$	4×10^4
8^b	14.5	DCB	Al	$1.8(\pm 0.3) \times 10^{-3}$	$3.5(\pm 0.2)$	1×10^4
8^b	15.0	CHCl_3	Al	$1.4(\pm 0.1) \times 10^{-3}$	$1.3(\pm 0.1)$	1×10^4
7^b	15.0	CHCl_3	Al	$4.0(\pm 0.5) \times 10^{-3}$	$0.7(\pm 0.4)$	1×10^4

^a: top-gate bottom-contact OFET, W/L: 2550 μm /180 μm (avg. 8 devices)

^b: bottom-gate top-contact OFET, W/L: 1200 μm /100 μm (avg. 4 devices)

6. X-ray Characterisation of Films

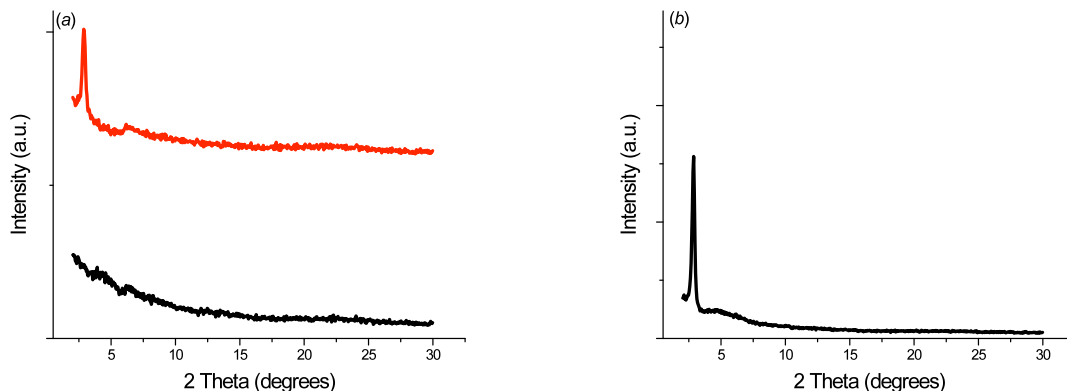


Figure S4. (a) XRD patterns of neat **7** films spin-coated onto glass substrates (Eagle 2000 Corning) from 1,2-dichlorobenzene (DCB) (above) and chloroform (below); (b) XRD pattern of neat **8** thin films spin-coating from 1,2-dichlorobenzene. The films cast from dichlorobenzene are somewhat crystalline, with Bragg peaks corresponding to d -spacings of 30.2° and 30.7° being seen for **7** and **8**, respectively, while the film cast from chloroform shows no evidence of crystallinity.

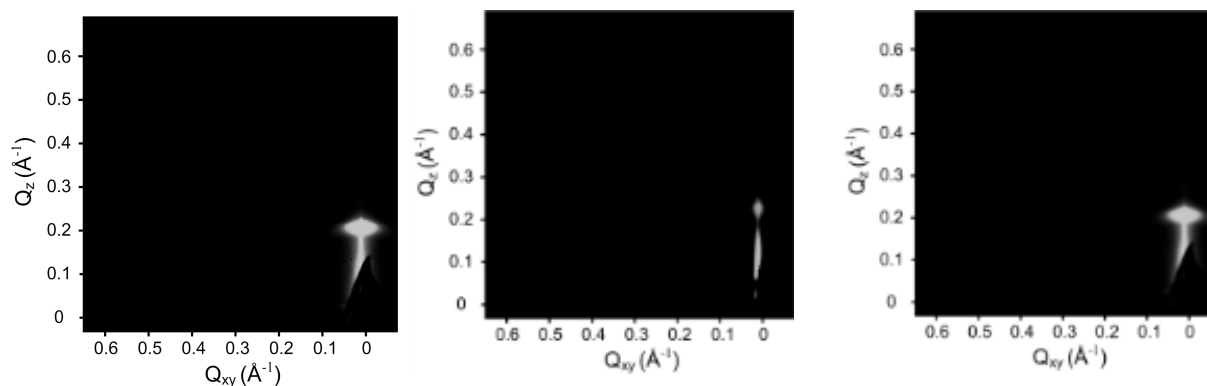
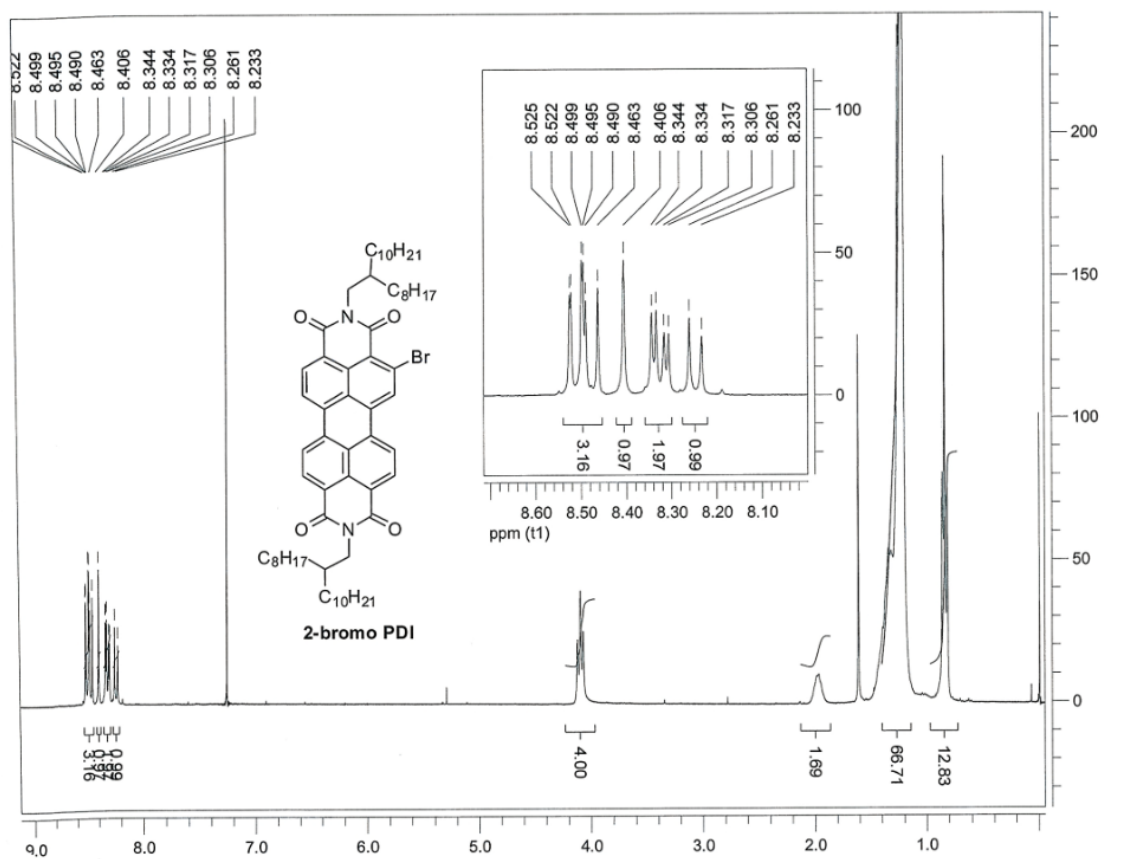


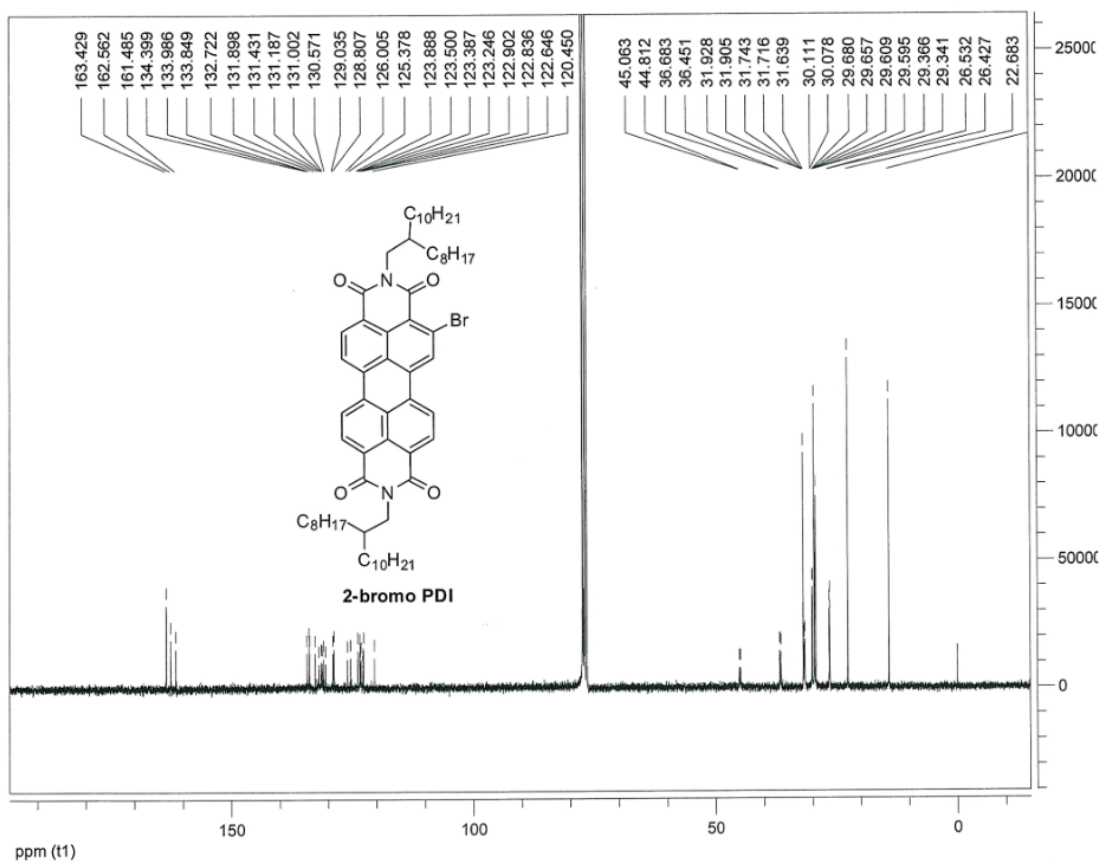
Figure S5. Grazing incidence wide angle x-ray scattering (GIWAXS) of thin films of triads coated onto glass substrates (Eagle 2000 Corning): **7** from DCB (left), **7** from chloroform (center), and **8** from DCB (right).

7. NMR Spectra of New Compounds

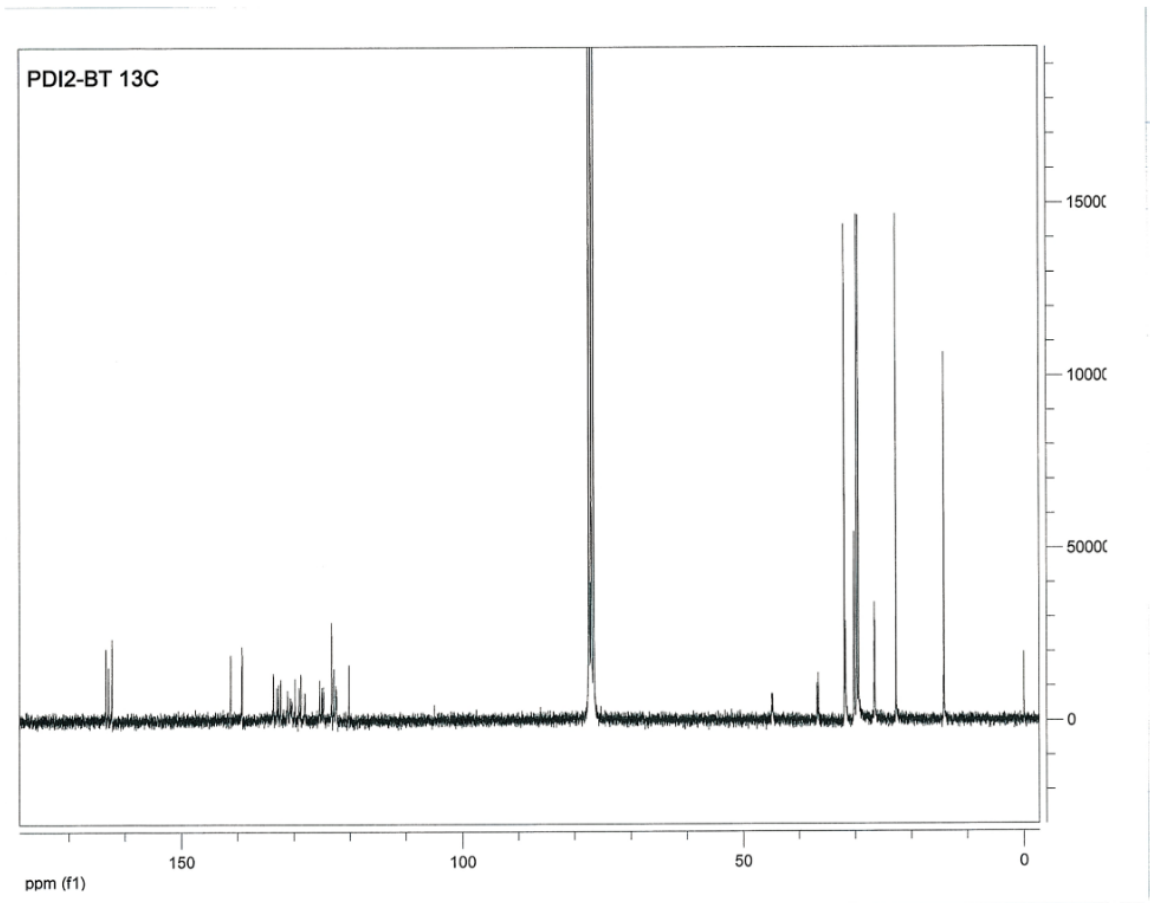
Compound 2



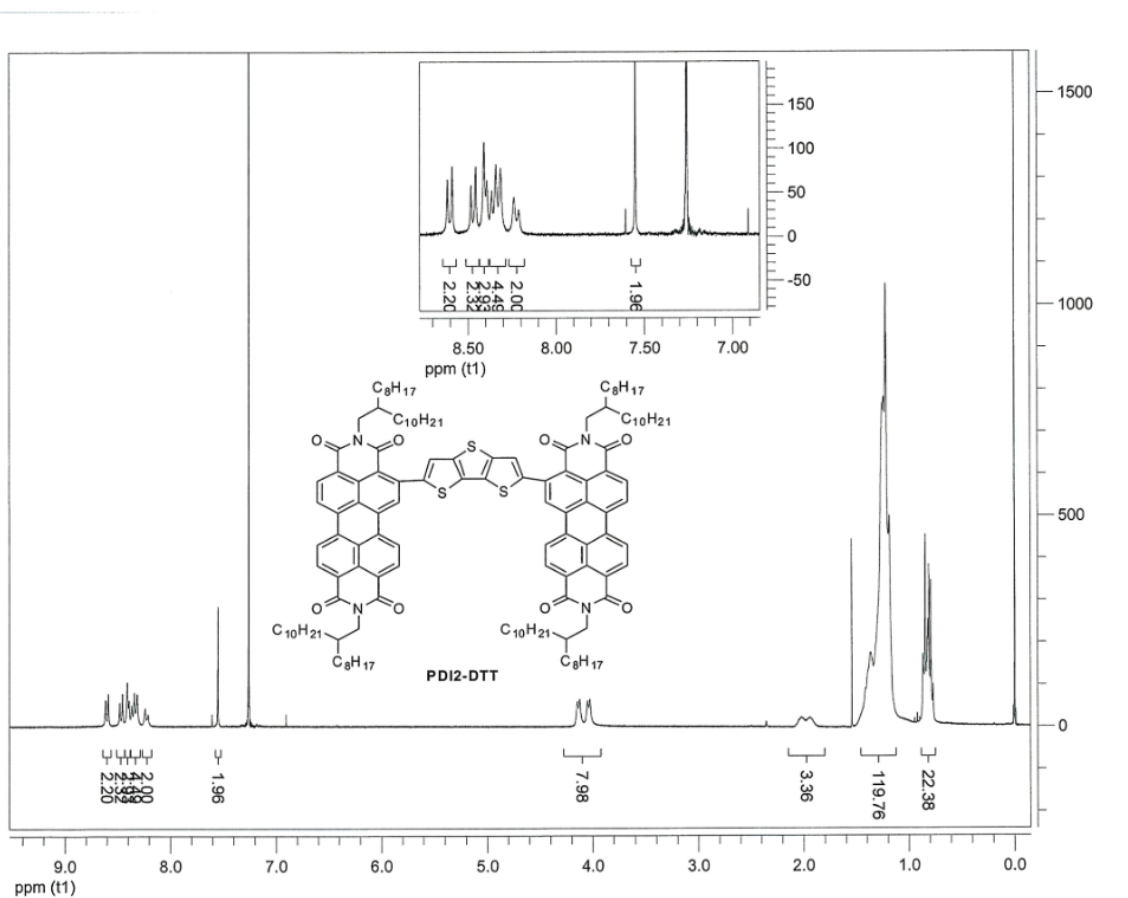
Compound 2



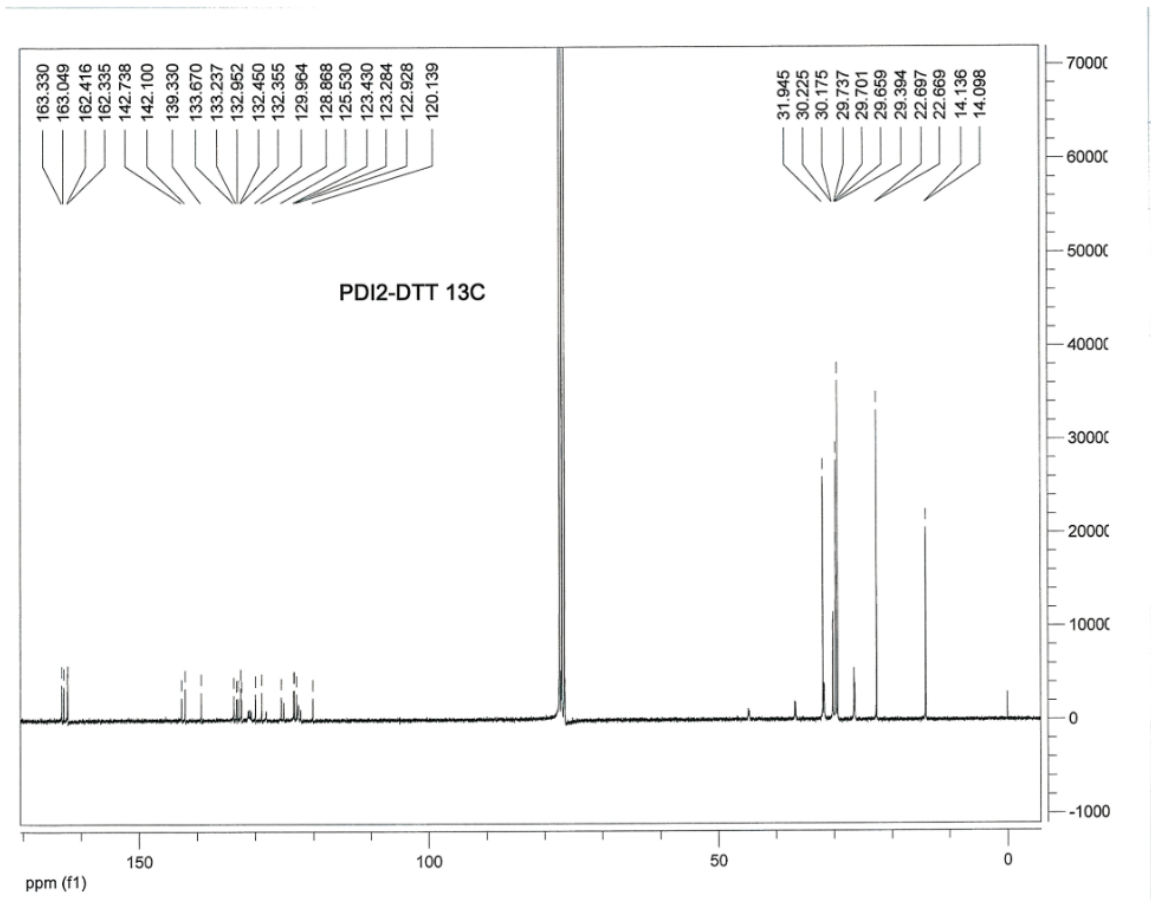
Compound 7



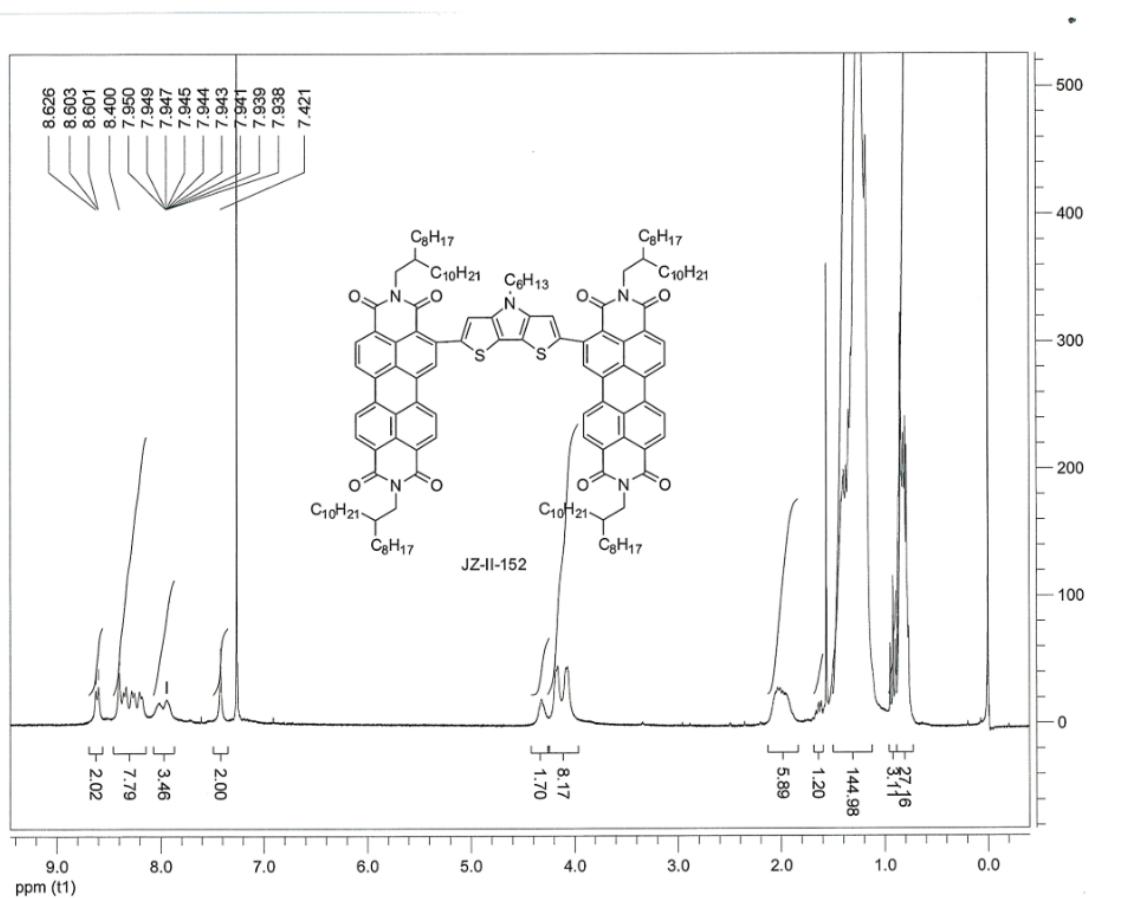
Compound 8



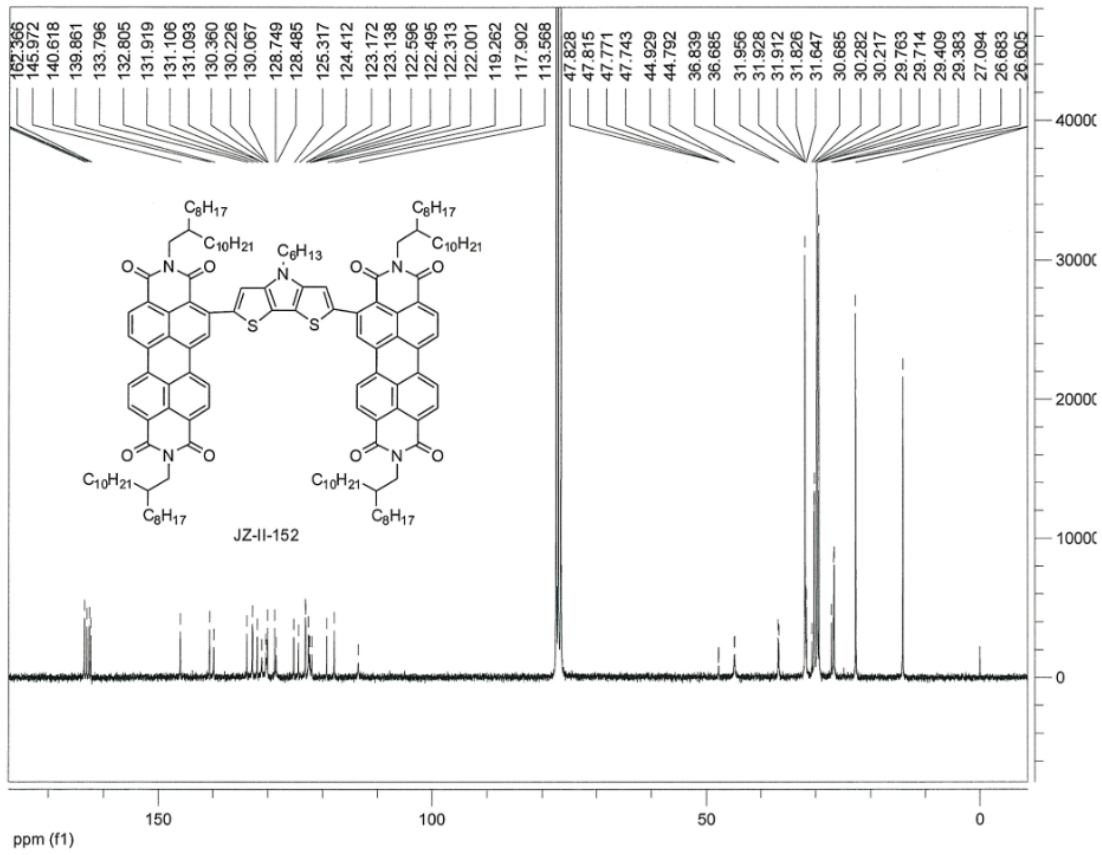
Compound 8



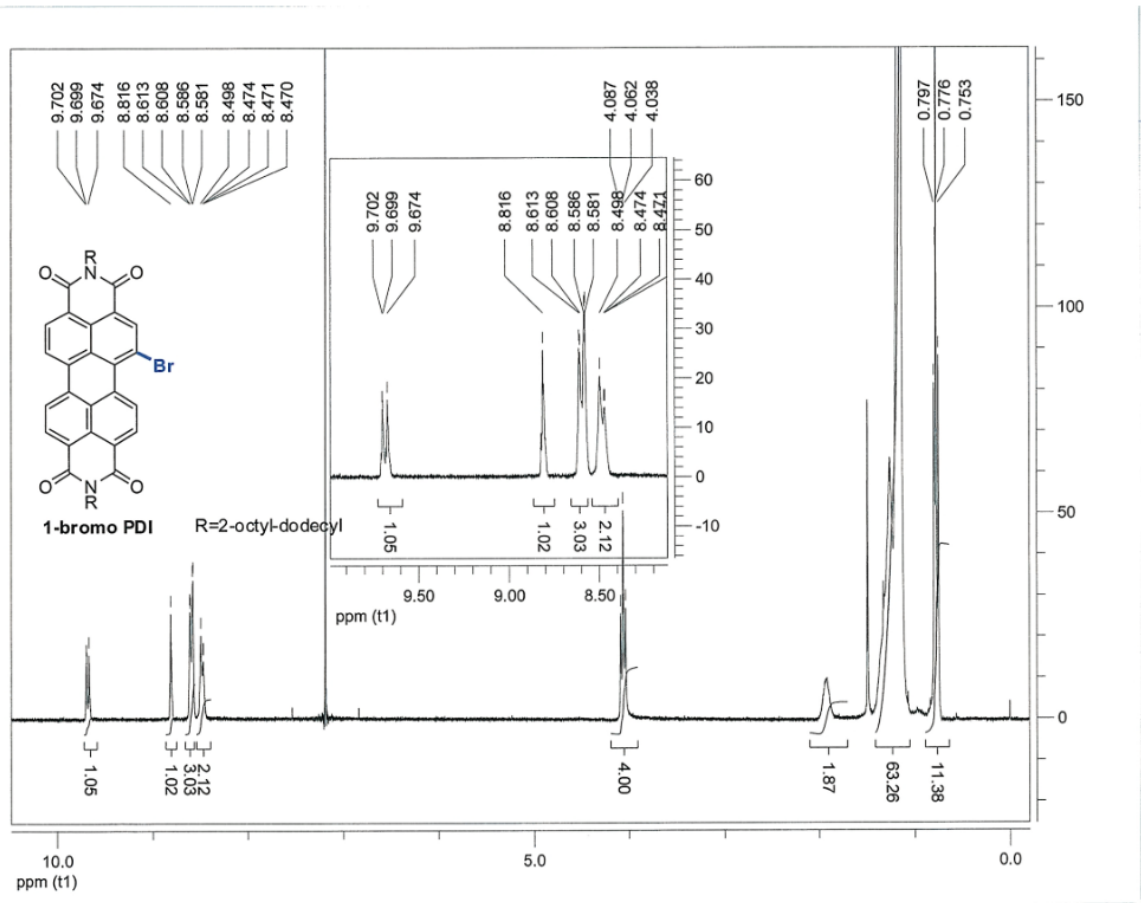
Compound 9



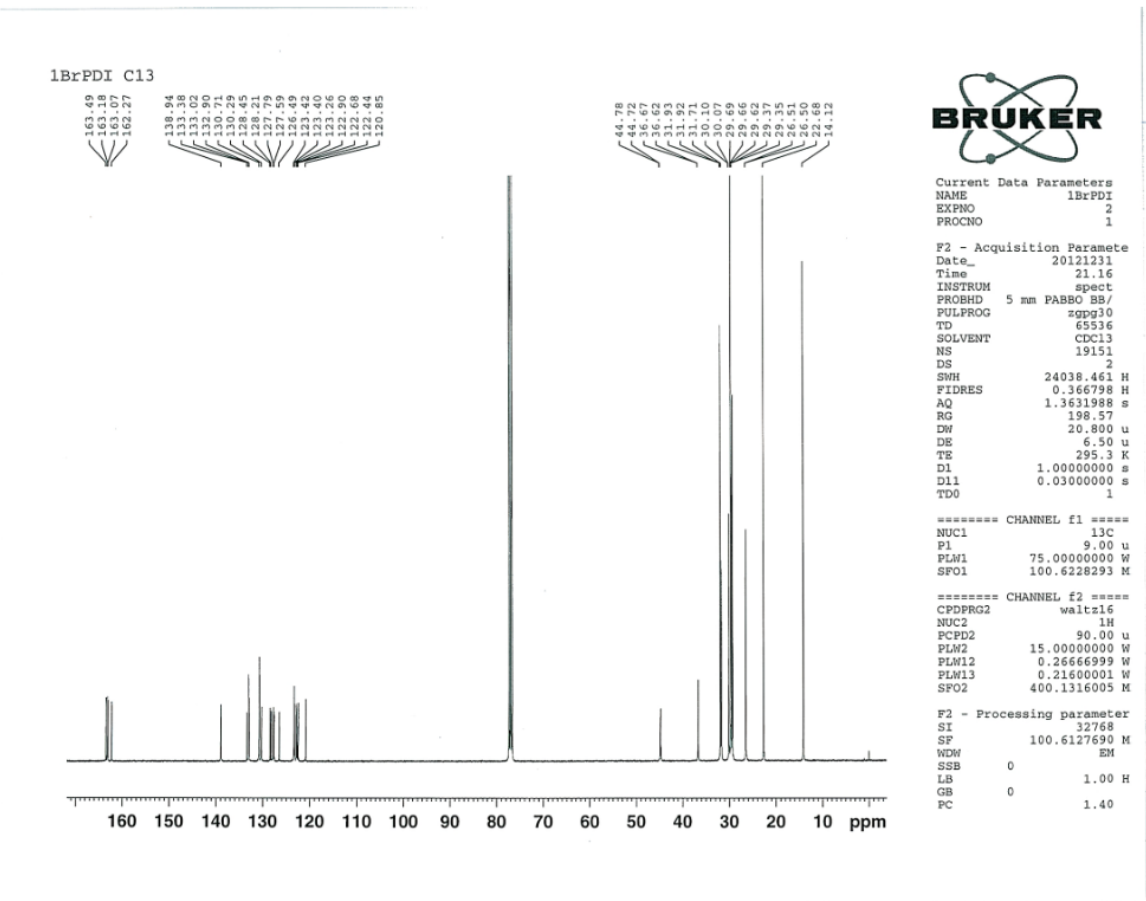
Compound 9



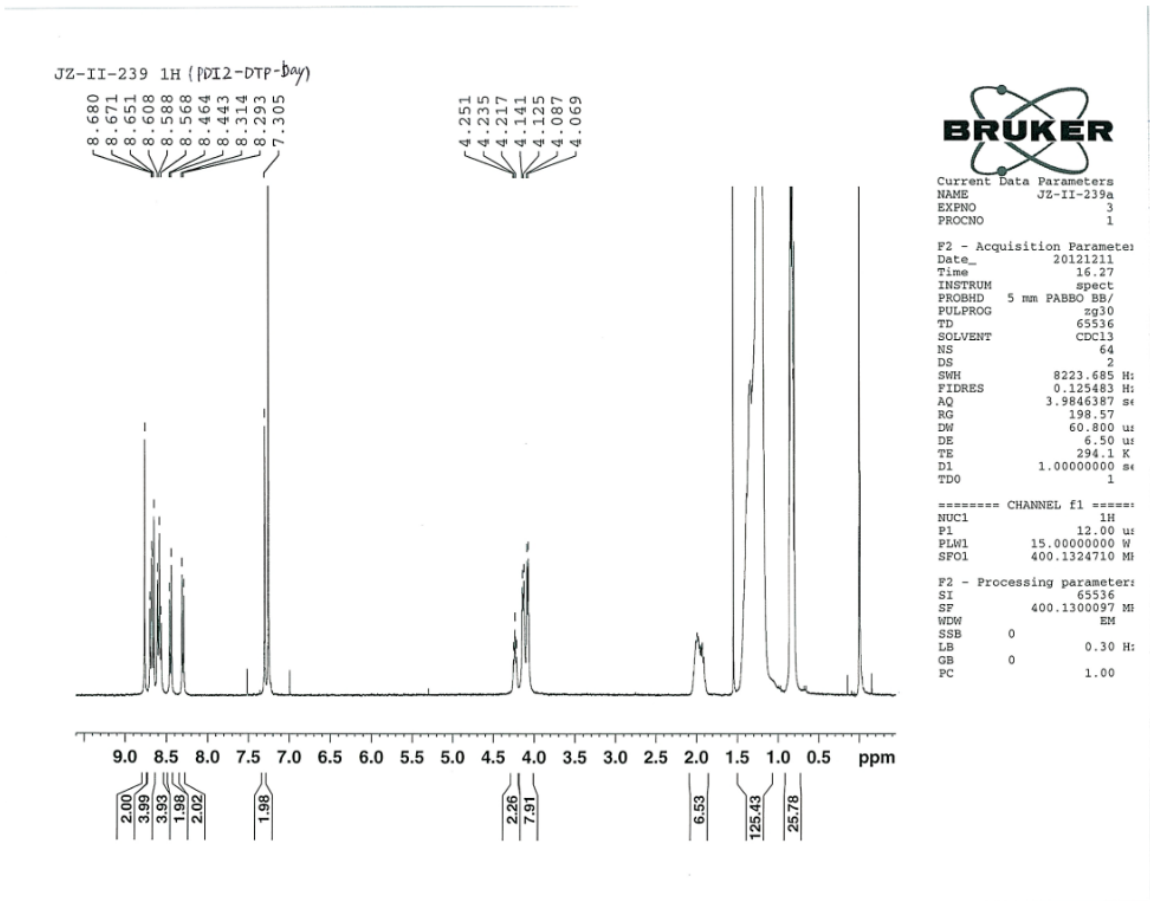
Compound 3



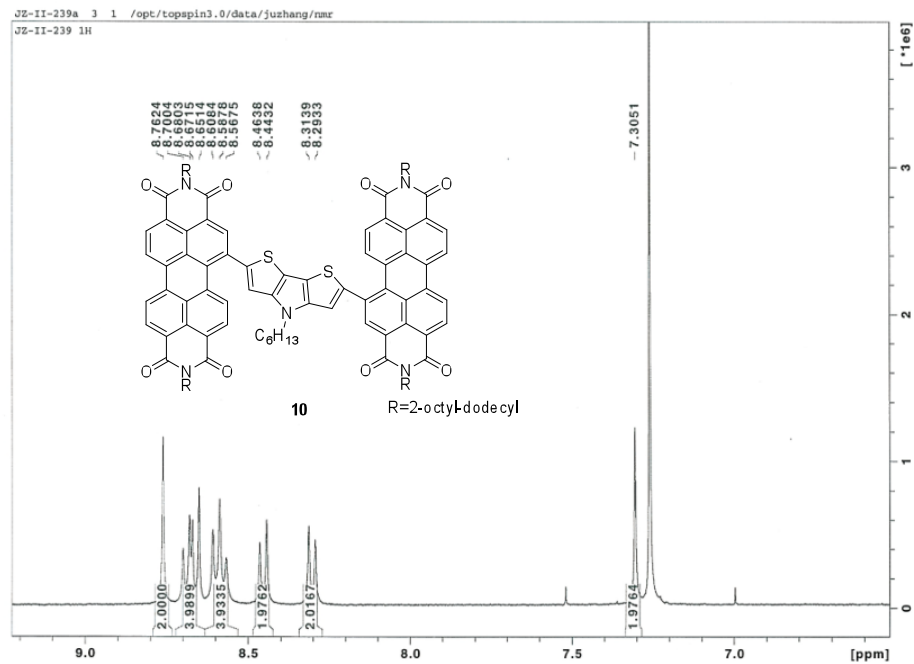
Compound 3



Compound 10



Compound 10



Compound 10

